

UC Davis

UC Davis Previously Published Works

Title

Biomembrane-Compatible Sol-Gel-Derived Photocatalytic Titanium Dioxide.

Permalink

<https://escholarship.org/uc/item/0wp0930t>

Journal

ACS applied materials & interfaces, 9(41)

ISSN

1944-8244

Authors

Johnson, Kaitlin E
Gakhar, Sukriti
Deng, Yue
et al.

Publication Date

2017-10-01

DOI

10.1021/acsami.7b12673

Peer reviewed

This document is confidential and is proprietary to the American Chemical Society and its authors. Do not copy or disclose without written permission. If you have received this item in error, notify the sender and delete all copies.

Biomembrane-Compatible Sol-Gel Derived Photocatalytic Titanium Dioxide

Journal:	<i>ACS Applied Materials & Interfaces</i>
Manuscript ID	am-2017-12673z.R1
Manuscript Type:	Article
Date Submitted by the Author:	n/a
Complete List of Authors:	Johnson, Kaitlin; University of California Davis, Department of Chemical Engineering Gakhar, Sukriti; University of California Davis, Department of Chemical Engineering Deng, Yue; University of California Davis, Chemical Engineering and Materials Science Fong, Keiko; University of California Davis, Department of Chemical Engineering Risbud, Subhash; UC Davis, Materials Science Longo, Marjorie; University of California Davis, Department of Chemical Engineering

SCHOLARONE™
Manuscripts

Biomembrane-Compatible Sol-Gel Derived Photocatalytic Titanium Dioxide

Kaitlin E. Johnson[‡], Sukriti Gakhar[‡], Yue Deng^{‡,†}, Keiko Fong[‡], Subhash H. Risbud[†], and
Marjorie L. Longo^{*,‡}

[‡]Department of Chemical Engineering, University of California Davis, Davis, California 95616,
United States

[†]Department of Materials Science and Engineering, University of California Davis, Davis,
California 95616, United States

ABSTRACT: Titanium dioxide gel monoliths were synthesized using an organic precursor and 0-30 vol% ethanol in water. The visible light-activated proton pump, bacteriorhodopsin, in its native purple membrane form, was successfully encapsulated within the titanium dioxide gels. Absorption spectra showed that the folded functional state of the protein remained intact within gels made with 0 and 15 vol% ethanol and retained the ability to make reversible conformational changes associated with the photocycle within the gel made with 0 vol% ethanol. The photocatalytic activity of gels made with no ethanol was significantly detectable and gels made with 0-30 vol% ethanol were comparable to commercial crystalline nanoparticles in similar solution conditions when irradiated with UV light. Our results show that sol-gel-derived photocatalytic titanium dioxide can be made biocompatible for a membrane-associated protein by minimizing the amount of ethanol and maximizing the amount of water in the synthesis procedure. The entrapment of the membrane protein, bacteriorhodopsin, in sol-gel derived

1
2
3 titanium dioxide provides the first step in future explorations of this bio-nanocomposite for
4
5 visible light photocatalysis, including hydrogen production.
6
7

8
9 **KEYWORDS:** amorphous titania, photocatalysis, water-splitting, bacteriorhodopsin, biohybrid
10
11 material
12

13 14 **INTRODUCTION**

15
16 Titania (titanium dioxide) has been studied widely for its photocatalytic capabilities in
17
18 addition to its many applications in technological products.¹⁻² From a fundamental standpoint,
19
20 electron-hole pairs form within the titania as a result of photon absorption under UV light.²
21
22 These charge carriers, if prevented from recombining, can then be used in redox reactions in
23
24 order to produce hydrogen through water-splitting. This presents the promising prospect for a
25
26 light-driven, environmentally-friendly fuel production process. Titania on its own is restricted to
27
28 light absorption from the UV range due to its large band gap, which prevents the practicality of
29
30 using titania in solar applications. As a result, research has focused on the sensitization of titania
31
32 in order to allow for excitation with visible light and therefore broaden its applications.³⁻⁷
33
34
35
36

37
38 The sensitization process in titania can be accomplished by using a dye species to absorb
39
40 visible light which can then inject an electron into the conduction band.⁷⁻⁸ Light-activated
41
42 proteins can also be used to achieve the same effect. One such protein, bacteriorhodopsin (BR),
43
44 functions as a proton pump across its native cell membrane in response to visible light in order to
45
46 assist in ATP synthesis in addition to its ability to act as a dye via a retinal cofactor.⁹⁻¹⁰ This
47
48 proton pump functionality is thought to be beneficial for photocatalytic applications as it may
49
50 help to transfer hydrogen ions to a reduction catalyst (typically platinum).³ In recent years, BR in
51
52 its native purple membrane environment has been successfully used in both photocatalytic and
53
54 photoelectrochemical applications to sensitize crystalline titania/platinum complexes.^{3, 5}
55
56
57
58
59
60

1
2
3 Crystalline titania often takes precedence over amorphous titania for the study and development
4
5 of photosensitive applications due to the larger band gap associated with amorphous titania as
6
7 well as the disorder inherent in the amorphous structure which may lead to more sites for
8
9 electron-hole pair recombination.^{1,11} Despite these limitations, amorphous titania is typically less
10
11 expensive and easier to fabricate and has a larger surface area, making it an attractive candidate
12
13 for photocatalysis.¹¹⁻¹³ However, to our knowledge, BR or any other integral membrane proteins
14
15 have not been incorporated into amorphous titania.
16
17
18
19

20
21 The present work is focused on the process development of amorphous photocatalytic
22
23 titania for encapsulation of BR and other integral membrane proteins through sol-gel synthesis.
24
25 We modify a popular sol-gel synthesis route for amorphous titania which is based on the
26
27 hydrolysis of an alkoxide titania precursor, followed by polycondensation to create a porous
28
29 polymeric or colloidal network called a gel. Monolithic gels were favored for this research rather
30
31 than amorphous nanopowder in order to maximize the surface area within a porous product. BR
32
33 could also be more easily incorporated into the monolithic gel as the pores would form around
34
35 the protein, circumventing the need for additional cross-linkers. We did not dry the sol-gel
36
37 monoliths as this would also decrease the available surface area provided by the pores as the
38
39 pores shrink from capillary stress.¹⁴⁻¹⁵ The procedure developed in this work can be easily
40
41 adapted to suit the creation of thin films through spin- or dip-coating for future applications
42
43 should such approach prove appealing in future work.
44
45
46
47
48

49
50 The use of ethanol as a solvent in the sol-gel process is a key concern of the research as
51
52 ethanol is frequently used in sol-gel processing to decrease gel time and increase surface area.
53
54 However, as high concentrations of alcohols are known to negatively impact the stability of both
55
56 BR and its native lipid bilayer environment,¹⁶ the ethanol content during synthesis was limited to
57
58
59
60

1
2
3 30 vol% or less. BR, associated with its native purple membrane, was incorporated into the
4
5 titania matrices and the stability of the protein within the gel environment was monitored over
6
7
8 time, including extended periods of high-intensity light exposure, and after light and dark
9
10
11 adaption in order to determine if BR retained its ability to undergo reversible conformational
12
13 changes associated with proton pumping. The photocatalytic activity of the titania under UV
14
15 irradiation was studied through the degradation of methylene blue and the performance was
16
17 compared to commercially available crystalline P25 titania nanoparticles in order to determine
18
19 the feasibility of amorphous titania monolithic gels as a photocatalyst comparable to materials
20
21 currently used for this purpose. Methylene blue was used a model organic molecule as it
22
23 degrades in the presence of species produced from the UV exposure of titania.^{11, 17-18}
24
25
26

27 **MATERIALS AND METHODS**

28
29
30 **Materials.** Titanium ethoxide (~80%), absolute ethanol, propylene oxide ($\geq 99.5\%$), methylene
31
32 blue ($\geq 82\%$), and crystalline P25 titanium dioxide nanopowder ($\geq 99.5\%$) were purchased from
33
34 Sigma-Aldrich, Inc. Hydrochloric acid (12.1M) was purchased from Aqua Solutions, Inc. (Deer
35
36 Park, TX). Purple membrane associated bacteriorhodopsin derived from *Halobacterium*
37
38 *salinarum* was purchased from Bras del Port, S.A. (Santa Pola, Alicante, Spain). A Barnstead
39
40 Nanopure System (Barnstead Thermolyne, Dubuque, IA) was used to purify water used in all
41
42 experiments.
43
44
45

46
47 **Synthesis of Amorphous Titania Gel Matrix.** During the typical synthesis of titania gels, 170
48
49 μL concentrated hydrochloric acid was added to 7-10 mL of DI water or diluted methylene blue
50
51 solution in the case of gels for photocatalytic characterization. This solution was then stirred
52
53 vigorously while a second solution of 1 mL titanium ethoxide and up to 3 mL absolute ethanol
54
55 was slowly dispensed into the stirred solution. The amount of ethanol used was varied to obtain
56
57
58
59
60

1
2
3 gels with concentrations of 70-100 vol% water. Once the titania precursor had been completely
4 incorporated, 1 mL of propylene oxide was added to the solution to encourage gelation. At this
5 point, the solution, or sol, was filtered using a 0.2 μm filter and dispensed into 3.5 mL acrylic
6 cuvettes, which were then sealed and stored in the dark, at room temperature to allow for
7 gelation. Gels typically solidified within 30 to 90 mins depending on water content with an
8 increase in gelation time with higher water content. The final transparent gels had a
9 concentration of approximately 0.28 M titania. Gels used for photocatalytic characterization
10 contained 17 μM methylene blue. As no ethanol was extracted from the gels, the final ethanol
11 concentration within the gel pores was determined through density measurements of the pore
12 liquid expelled as gels were allowed to age and harden over the course of 1-7 days while covered
13 at room temperature and in the dark (see Supporting Information). To consider the effects of
14 porosity and ethanol concentration on the level of photocatalytic activity achieved by the titania
15 gels, additional gels were developed (see Supporting Information).
16
17
18
19
20
21
22
23
24
25
26
27
28
29
30
31
32
33

34 **Bacteriorhodopsin Encapsulation.** Titania gels for BR encapsulation were synthesized
35 following protocols described in the synthesis section with DI water replacing the methylene
36 blue solution. BR suspended in ultra-pure DI water was added to the titania sol once the sol had
37 been filtered as previously described. The sol with a final BR concentration of 5 μM , was gently
38 mixed and allowed to gel while sealed and covered on the benchtop. Gelation typically occurred
39 within 30 to 60 mins and the transparent gels were stored in the dark at 4°C for at least 20 days.
40
41 Temperature-dependent visible spectra of the gel-encapsulated BR was measured using a UV-
42 2450 UV/Vis spectrophotometer (Shimadzu Corp., Kyoto, Japan). To determine the stability of
43 BR in solution or when encapsulated in titania gels, samples were irradiated with 365 nm light
44 from a Spectroline ENF-280C dual-wavelength UV lamp (Spectronics, Corp., Westbury, NY) or
45
46
47
48
49
50
51
52
53
54
55
56
57
58
59
60

1
2
3 a UVL-21 UV Lamp (UVP, LLC., Upland, CA) at an intensity of 1.80 ± 0.01 mW/cm². For trials
4 involving 435-700nm white light, 100mW/cm² light was generated using a 300W Lambda LS-
5
6
7
8 XL xenon arc lamp (Sutter Instrument Co., Novato, CA) with a 435nm longpass filter (Chroma
9
10
11 Technology Corp., Bellows Falls, VT) and heat-absorbing glass (Edmund Industrial Optic Inc.,
12
13 Barrington, NJ). The intensity of the white light was monitored using a LED light meter (FLIR
14
15 Systems, Inc., Wilsonville, OR).
16

17
18 **Characterization of Titania Gels.** Wet gels are challenging to characterize fully using
19
20 conventional methods as drying the gels will result in significant changes to the gel's structure as
21
22 the pores within it will shrink in response to the capillary pressure during solvent extraction.¹⁴⁻¹⁵
23
24 To overcome this difficulty, the porosity of the gels was characterized by monitoring the volume
25
26 loss of pore liquid during expedited ageing. During the ageing process, the pores within the gel
27
28 will collapse as the surface groups undergo condensation, causing the pore liquid to be excreted
29
30 from the gel in a process called syneresis.¹⁴ The ageing behavior of the gels was artificially
31
32 accelerated by heating the gels at 85°C. Every hour, the excreted pore liquid was removed from
33
34 the gel container and the mass of the hardened gels were measured to monitor pore liquid loss.
35
36 This monitoring of the ageing gels continued until pore liquid was no longer expelled from the
37
38 gel. Using recorded values of pore liquid density (see Supporting Information), the amount of
39
40 volume in the gel filled with pore liquid was determined in order to calculate the amount of
41
42 porosity within the gels.
43
44
45
46
47

48
49 **Photocatalytic Activity.** Titania gels containing methylene blue were irradiated from above in
50
51 the dark with 365 nm light from a Spectroline ENF-280C dual-wavelength UV lamp
52
53 (Spectronics, Corp., Westbury, NY) and a UVL-21 UV Lamp (UVP, LLC., Upland, CA) at an
54
55 intensity of 1.80 ± 0.01 mW/cm² for 1 to 5 hours at a time. The intensity of the light irradiating
56
57
58
59
60

1
2
3 samples was regularly monitored using a UV512AB Digital UV AB Light Meter (General Tools
4 & Instruments, LLC., New York). Photocatalytic activity in the gels was compared with the
5 behavior of crystalline P25 nanopowder. The powder was suspended in a solution of methylene
6 blue and water with the same titania, dye, and ethanol concentration as the gels and the slurry
7 was mixed while irradiated from above under the same light conditions as the gels following 90
8 mins of mixing in the dark to ensure maximum dye adsorption to the particles. A SpectraMax
9 M2 UV/Vis spectrophotometer (Molecular Devices, LLC., Sunnyvale, CA) was used to
10 determine the absorbance of all samples before and after UV irradiation. Degradation of the
11 methylene blue within samples was calculated by monitoring the peak height at 665 nm as this is
12 directly proportional to the concentration of methylene blue through the Beer-Lambert Law.
13
14
15
16
17
18
19
20
21
22
23
24
25
26

27 **RESULTS AND DISCUSSION**

28
29 **Presence of Titania in Gels.** Titania gels were synthesized as monoliths from a titanium
30 ethoxide precursor in an aqueous environment containing 0, 15, or 30 vol% ethanol in order to
31 provide a range of biomembrane compatibility from highest to lowest. The gels were visibly
32 transparent, indicating there was minimal to no light scattering in the gels which we attribute to a
33 filtration step in the synthesis. UV/Visible spectra of all monolithic gels before UV irradiation
34 displayed significant absorbance in the 250-375 nm region associated with the presence of
35 titanium dioxide as shown in Figure 1. The titania peak onset or cut-off wavelength, as
36 determined graphically through inspection of UV/Vis spectroscopy data, was used to calculate
37 the band gap of the amorphous gels (see Supporting Information). With an average onset
38 wavelength of 365.9 ± 0.5 nm, the band gap of the titania gels was calculated as 3.39 ± 0.01 eV.
39
40
41
42
43
44
45
46
47
48
49
50
51
52
53
54
55
56
57
58
59
60

onset wavelength of 377.8 ± 1.4 nm and a band gap of 3.28 ± 0.01 eV. The determined band gap values of the sol-gel-derived titania as well as the crystalline P25 nanopowder fall within the typical range of values seen in previous studies.^{4, 11, 18-20} Amorphous titania had a 3% increase in band gap energy compared to the crystalline P25. This increase in band gap energy is typical of amorphous sol-gel titania.¹⁹

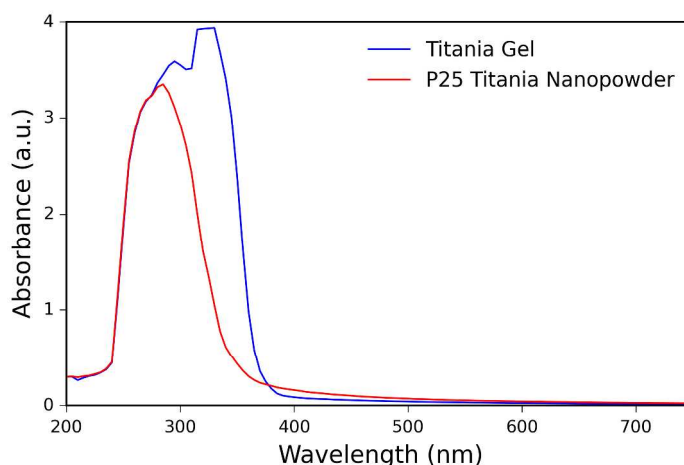


Figure 1. UV/Visible spectrum of a typical monolithic gel, demonstrated with a gel made in 100 vol% water. By comparison, P25 crystalline nanopowder in water is shown. The 250-375 nm region is associated with the presence of titanium dioxide and no peaks are present in the visible range.

Characterization of Titania Gels and Pore Liquid. Density measurements of pore liquid during natural ageing were used to determine the final ethanol concentration within the developed titania gels in order to assess biomembrane compatibility. The calculated final ethanol concentration in the pore liquid for each gel synthesis is shown in Table 1. Determining the final ethanol concentration within the pores of the gels is essential to determine the environment that will impact any biomolecules encapsulated within the gels. Additionally, the ethanol concentration will have a significant impact on the photocatalytic activity of the gels. The

1
2
3 ethanol concentration in the pores of the 100 vol% water gels was 0.8 M, which is due to ethanol
4 production during hydrolysis and potentially condensation reactions during the synthesis.
5
6 Despite the relatively large error bounds, 0.8 M ethanol is stoichiometrically consistent with
7
8 nearly complete conversion of the titanium ethoxide precursor to 0.28 M TiO₂ as four ethanol
9
10 molecules would be present for every titanium atom.
11
12
13
14

15 **Table 1.** Porosity and Ethanol Concentration in Pores of Synthesized Gels
16

Gel	Final Ethanol Concentration	Porosity
70 vol% Water	11.4±1.4 M	86±5%
85 vol% Water	6.4±3.5 M	87±4%
100 vol% Water	0.8±1.5 M	81±3%

17
18
19
20
21
22
23
24
25
26
27 The porosity of the gels, measured through encouraged ageing, is shown in Table 1. The
28
29 70 and 85 vol% water gels achieved a porosity of 86±5% and 87±4%, respectively. Such a level
30
31 of porosity is consistent with what would be expected in gels prior to solvent extraction.¹⁴⁻¹⁵ 100
32
33 vol% gels had a porosity of 81±3%, likely due to the fact that higher concentrations of water
34
35 result in higher rates of hydrolysis and crosslinking which are associated with materials of a
36
37 lower surface area and porosity.^{15, 21-22} The difference in the level of porosity achieved by the 70
38
39 and 85 vol% water gels and the 100 vol% water gels was statistically significant (see Supporting
40
41 Information) and is important for future considerations in gel synthesis as higher surface area
42
43 will provide advantages in photocatalytic applications.
44
45
46
47

48
49 **Encapsulation of Bacteriorhodopsin in Gels.** Bacteriorhodopsin in purple membrane was
50
51 encapsulated in the titania gels through addition of the protein and gentle mixing during the
52
53 gelation stage, following filtration of the sol. The presence of BR in a functional conformation in
54
55 titania gels was confirmed through UV/Vis spectroscopy. When BR is properly folded in
56
57
58
59
60

1
2
3 association with its retinal chromophore, the molecule responsible for photon absorption, the
4 protein will have an absorbance maximum around 560-570 nm.²³⁻²⁵ In the case of BR
5
6 denaturation, this retinal peak will shift to 380-400 nm as the tertiary structure of the protein
7
8 deteriorates and the retinal is stripped from the structure.²³⁻²⁴ The absorbance spectra of the
9
10 titania gels with encapsulated BR are compared to the spectra from BR in solution with ethanol
11
12 concentrations matching that of the pore liquid in each set of gels in Figure 2.
13
14
15
16

17
18 The BR in both solution and within the titania gels undergoes increasing amounts of
19
20 denaturation as a result of increasing ethanol concentrations as apparent by the decrease in
21
22 absorbance at 555-560 nm and increase at 400 nm. These results are consistent with previous
23
24 studies which have observed the same trend of BR in ethanol as alcohols disrupt the hydrogen
25
26 bonding within the tertiary structure of the protein.²³⁻²⁴ Background spectra from titania gels
27
28 without protein was minimal between 360 and 700 nm and it was removed from the spectra of
29
30 gels encapsulating BR in order to isolate the effects from the protein. As shown in Figure 2A, the
31
32 peak absorbance of the BR within the 100 vol% water gel occurs in close proximity to that of the
33
34 properly folded BR in solution (555 nm for gel and 560 nm for solution) and the peak itself is
35
36 clearly defined with a shape matching that of the properly folded BR in solution. There also
37
38 appears to be a sub-population of denatured BR indicated by a similar absorbance at 360 nm.
39
40
41 Gels made with 15 vol% ethanol (85 vol% water) showed evidence of less properly folded BR
42
43 and more denatured BR in the absorbance. In the presence of 11.4 M ethanol, BR in solution and
44
45 in the gel (70 vol% water gel) appears to be fully denatured. These trends are also shown by
46
47 visual inspection of the titania gels as shown in Figure 3, wherein the 100 vol% water gel
48
49 maintains the pink-purple color indicative of the presence of properly folded BR while the 85
50
51 and 70 vol% water gels show decreasing amounts of pink coloration.
52
53
54
55
56
57
58
59
60

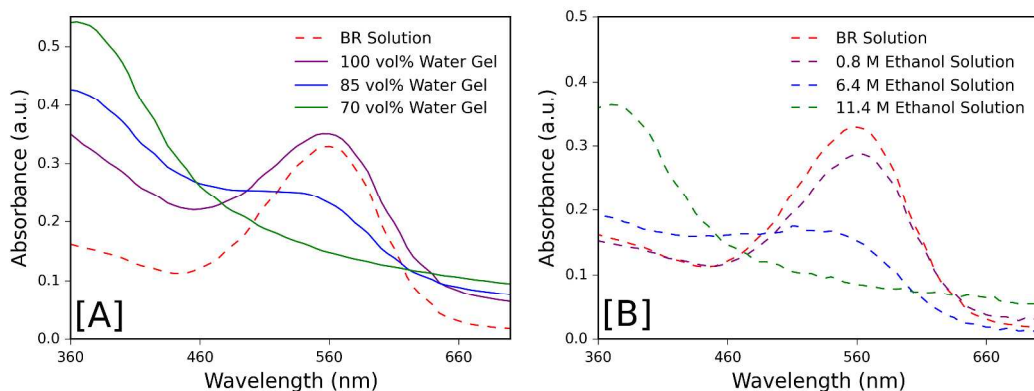


Figure 2. Visible range spectra of (A) titanium dioxide gels with encapsulated bacteriorhodopsin and (B) bacteriorhodopsin solution with varying concentrations of ethanol matching the measured concentrations of the gels. For the gels, the volume percentage of water used during synthesis is indicated. Background from empty titania gels with corresponding water concentrations was removed from the spectra. The 555 and 560 nm absorbance indicates the concentration of stable BR within the gel.

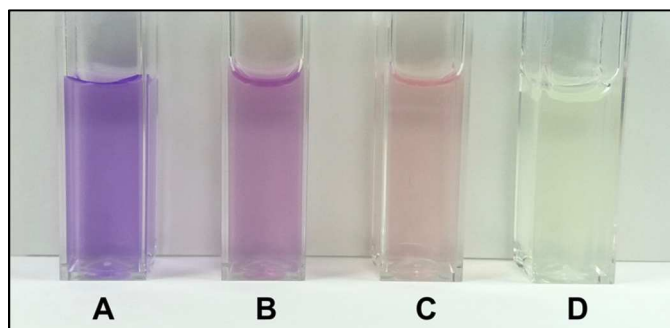


Figure 3. Encapsulation effect on the pink-purple coloration of bacteriorhodopsin in (A) aqueous solution (no encapsulation or ethanol), (B) 100 vol% water titanium dioxide gel, (C) 85 vol% water titanium dioxide gel and (D) 70 vol% water titanium dioxide gel. The remainder of the solvent used in the synthesis was ethanol.

1
2
3 Overall, BR encapsulated in titania gels results in higher absorbance values than that seen
4 in solution, likely due to a small amount of scattering from the gel matrix. While the background
5 absorbance of the titania gels was minimal in the visible light region and was removed for the
6 purpose of data analysis, the onset of the UV-range titania peak resulted in data too noisy for
7 accurate analysis between 300-360 nm. The peak from denatured BR retinal in the gels (360-370
8 nm) may have been exaggerated to some extent due to its close proximity to the titania peak and
9 scattering.
10
11
12
13
14
15
16
17
18

19
20 To determine the stability of the membrane protein in titania, the absorbance of the
21 encapsulated BR was monitored over the course of two weeks through observation of the BR
22 peak (550-560 nm) in the visible range. BR within 100 vol% water gels underwent an average
23 peak height change of $0.2 \pm 0.8\%$ after two weeks of encapsulation and storage at 4°C and no
24 evidence of significant gel shrinkage or damage from solvent loss was found through visual
25 inspection of the gels containing BR. The demonstrated stability of both the protein and the gel is
26 promising for longer term encapsulation of a membrane protein within amorphous titania.
27
28
29
30
31
32
33
34
35

36 BR in solution and encapsulated within titania gels was exposed to high intensity UV and
37 white light (435-700 nm) for at least five hours and the change in retinal absorbance (555 nm for
38 gel and 560 nm for solution) was monitored in order to determine the robustness of the BR under
39 irradiation and indicate the feasibility of future application in hydrogen production. When in
40 solution, the BR experienced a $1.21 \pm 0.43\%$ and $0.13 \pm 0.09\%$ relative loss in peak height
41 following irradiation with UV and white light respectively. When encapsulated, there was a
42 relative peak height loss of $3.71 \pm 0.02\%$ with UV light and $3.42 \pm 1.82\%$ with white light. The
43 difference in level of peak degradation between solution and gel samples was determined to be
44
45
46
47
48
49
50
51
52
53
54
55
56
57
58
59
60

1
2
3 statistically significant (see Supporting Information) and is likely due to the presence of ethanol
4
5 within the gel.
6
7

8
9 Ethanol has positive effects on both the properties and the photocatalytic capabilities of
10 the final gel product. However, the negative impact that even small amounts of ethanol used
11 during gel synthesis has on the stability of the BR in the gel cannot be ignored. Therefore, future
12 research and development will need to focus on lessening the deterioration of the BR without a
13 significant sacrifice to the photocatalytic activity of the final product. Adding small amounts of
14 ethanol or methanol below the concentration threshold that leads to severe BR degradation to the
15 100 vol% water sol is a promising option for increased photocatalytic activity without sacrificing
16 protein content. Using methanol would likely improve the performance of the gels as it is a more
17 efficient sacrificial electron donor (SED) than ethanol²⁶ and requires higher concentrations than
18 ethanol to achieve the same level of BR denaturation.²³
19
20
21
22
23
24
25
26
27
28
29
30
31

32 **Bacteriorhodopsin Functionality within Titania Gels.** In order to study the functionality of the
33 BR when encapsulated in titania, the capability of the protein to make the conformational
34 changes necessary to convert between dark- and light-adapted states was monitored using
35 UV/Vis spectroscopy. Dark-adapted BR when not exposed to light exists in a mixture of 13-*cis*-
36 retinal and all-*trans*-retinal conformations and have a maximum absorbance around 558-560
37 nm.^{25, 27} In order to initiate the photocycle responsible for proton pumping, BR must first be
38 converted to an all-*trans*-retinal conformation by absorbing light.^{25, 27-30} This light-adapted state
39 is characterized by a small red-shift in the maximum absorbance of the protein to around 568
40 nm.^{25, 27} Evidence of this state conversion with BR encapsulated in titania will be an indication of
41 protein functionality and the feasibility of taking advantage of BR's proton pumping function for
42 water-splitting applications. The absorbance of BR in aqueous solutions and encapsulated in 100
43
44
45
46
47
48
49
50
51
52
53
54
55
56
57
58
59
60

1
2
3
4
5
6
7
8
9
10
11
12
13
14
15
16
17
18
19
20
21
22
23
24
25
26
27
28
29
30
31
32
33
34
35
36
37
38
39
40
41
42
43
44
45
46
47
48
49
50
51
52
53
54
55
56
57
58
59
60

vol% water gels were measured after each sample had been isolated in the dark from all light for several hours. It was then exposed to white light (435-700 nm) for an additional absorbance measurement before being once again isolated in the dark prior to a final absorbance spectra. This process allowed for the extent of the light-adapted state red-shift as well as the reversibility in each sample medium to be analyzed. The absorbance transition in the gel and in solution is shown in Figure 4.

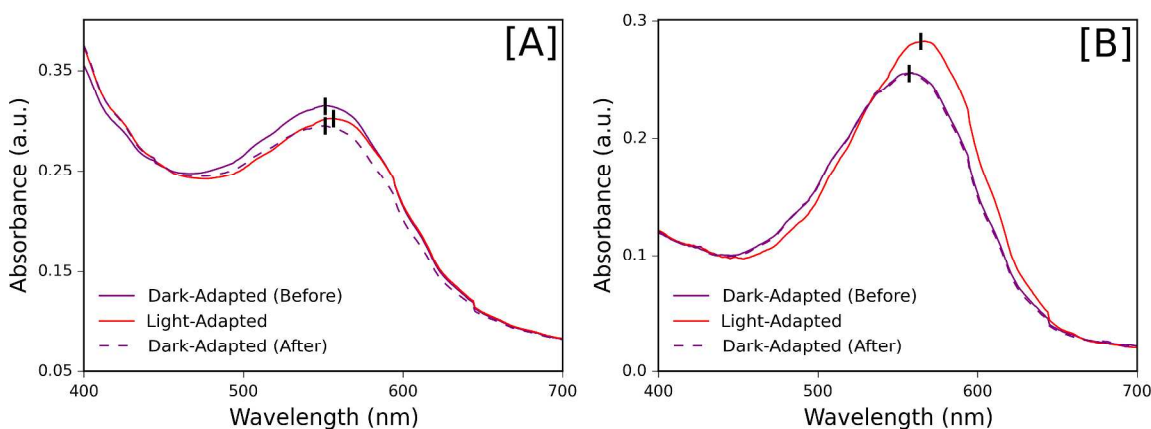


Figure 4. Visible absorbance spectra of dark (before and after light-adaption) and light-adapted state bacteriorhodopsin when (A) encapsulated in titania gels and (B) when in solution. The maximum absorbance peak for each spectrum is indicated by a vertical line.

The maximum absorbance peak of the encapsulated BR achieved a red-shift of 5.1 ± 0.2 nm when converting from the dark- to the light-adapted state. When in solution, BR underwent a red-shift of 7.1 ± 0.3 nm. While the magnitude of the red-shift appear statistically significant between the gel and solution (see Supporting Information), this difference may be due to influence of the ethanol-denatured BR (360 nm) peak on the spectra and upon deconvolution, the two may be nearly indistinguishable. That the encapsulated BR was capable of accomplishing a reversible red-shift indicates that the protein appears functional while confined within the gel and

1
2
3 this is a promising indication that completion of the proton pumping photocycle can occur in the
4
5 gel.
6
7

8 While both the BR conformational transition in titania and in solution were shown to be
9
10 reversible in that the maximum absorbance returned to the dark-adapted wavelength following
11
12 light-adaption, the encapsulated protein did have a decrease in absorbance at this wavelength.
13
14 This decrease was coupled with an increase in absorbance of the 360 nm peak indicating further
15
16 protein denaturation. This apparent degradation following light-adaption may be due to the
17
18 presence of ethanol in the gel and an increased vulnerability of the protein to deterioration due to
19
20 the conformational change.
21
22
23

24 An increase in temperature is known to cause changes in BR's visible spectra as the
25
26 protein's secondary structure shifts in response to the temperature change.²⁴ The retention of this
27
28 thermochromic functionality of BR under confinement was observed within titania gels made
29
30 with 100 vol% water. As shown in Figure 5, the titania-encapsulated BR undergoes a progressive
31
32 blue-shift of 10.1 ± 0.3 nm with a temperature increase from 10°C to 50°C. BR when under no
33
34 encapsulation in aqueous solution was found to have a blue-shift of 9.5 ± 0.1 nm under the same
35
36 temperature increase (see Supporting Information). The difference between the magnitude of
37
38 blue-shift when the BR was free in solution and encapsulated in titania was not found to be
39
40 statistically different (see Supporting Information). The extent of thermochromic behavior of BR
41
42 encapsulated in our titania gels is comparable to work conducted by Neebe et al²⁴ wherein BR
43
44 was encapsulated in polyacrylamide gels and thin films. Gels made with 85 vol% water did not
45
46 have enough of a distinguishable BR peak to successfully monitor any thermochromic behavior.
47
48
49
50
51
52
53
54
55
56
57
58
59
60

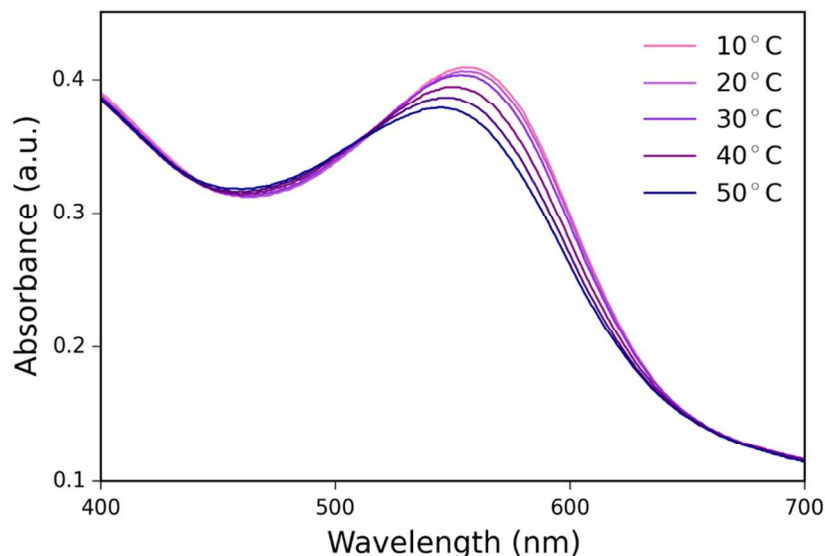


Figure 5. Temperature-dependent absorbance shift of bacteriorhodopsin encapsulated within a titanium dioxide gel made in 100% water following background removal of titania from spectra.

That the BR is able to maintain its thermochromic behavior from within the 100 vol% water titania gel indicates the retention of appropriate folding, the retention of the retinal cofactor, and the retention of its surrounding membrane, in addition to the likelihood of the retention of other functionalities while encapsulated. The proton-pumping behavior of BR requires conformational changes, as the retinal isomerization allows for deprotonation of the protein.^{10, 31} Freedom of motion during entrapment is therefore essential in order to take advantage of BR as a proton pump in future applications to increase hydrogen production during photocatalysis.

Photocatalytic Activity of Titania Gels. Titania gels were synthesized as monoliths from a titanium ethoxide precursor in an aqueous environment containing 0, 15, or 30 vol% ethanol and 17 μ M methylene blue dye in order to confirm that the gels of varying biomembrane compatibility were photocatalytic. Irradiation by UV light of 365 nm wavelength had no

1
2
3
4
5
6
7
8
9
10
11
12
13
14
15
16
17
18
19
20
21
22
23
24
25
26
27
28
29
30
31
32
33
34
35
36
37
38
39
40
41
42
43
44
45
46
47
48
49
50
51
52
53
54
55
56
57
58
59
60

significant effect on the titania absorbance in the gels and only resulted in a decrease of the methylene blue absorbance peak height at 665 nm (see Supporting Information). The normalized concentration of methylene blue was calculated by monitoring the peak height at 665 nm, as this is directly proportional to the concentration of methylene blue. Photocatalytic activity of the gels was studied by comparing the methylene blue concentration loss in the UV-irradiated gels over time. As shown in Figure 6, titania gels displayed methylene blue degradation trends similar to that obtained with commercial crystalline P25 nanopowder of the same titania and ethanol concentrations in water. After five hours of UV treatment, 85 vol% water gels showed a $91.6 \pm 3.5\%$ degradation. Gels with 70 vol% water experienced similar performance (see Supporting Information). Titania gels made with 100 vol% water had about 50% less methylene blue degradation than the 85 vol% water gels as shown in Figure 6. This is also indicated by visual inspection of the gels in Figure 7 as the 85 vol% water gels can be seen to achieve the higher degrees of methylene blue degradations with gels appearing colorless after about four hours of UV irradiation. It should be noted that there was no methylene blue degradation in titania gels or when in contact with crystalline P25 when stored in the dark and not subjected to UV irradiation.

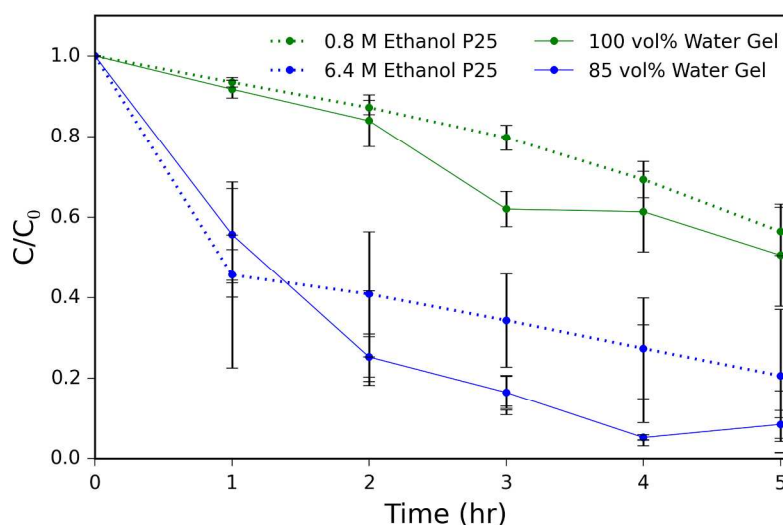


Figure 6. Methylene blue degradation in titanium dioxide gels over time from UV irradiation.

C/C_0 represents the methylene blue concentration post UV irradiation normalized by the concentration prior to UV irradiation. Given are the volume percentage of water used in the sol-gel synthesis; the remainder was ethanol. Crystalline P25 titanium dioxide nanoparticles were suspended in water and ethanol solutions that matched the measured ethanol contents of the gels.

Error bars represent the standard deviation.

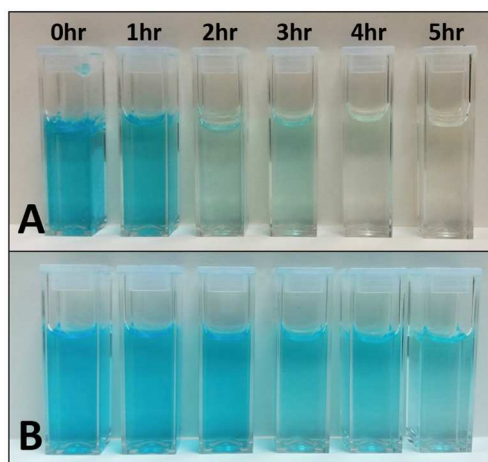


Figure 7. Progression of methylene blue degradation due to UV exposure in titanium dioxide gels made in (A) 85 vol% water gels and (B) 100 vol% water gels. The remainder of the solvent used in the synthesis was ethanol.

The extent of methylene blue degradation increases with increasing amounts of ethanol in the gel. Short-chain alcohols such as ethanol, are well-known to aid photocatalysis as a sacrificial electron donor, resulting in higher photocatalytic activity in association with titania.^{3, 7, 26, 32-33} In this case, the excess ethanol functions as a reducing agent within the system and is oxidized by the holes generated within the titania as a result of light irradiation³³ as shown in Figure 8. As the holes are consumed by the oxidation reaction with the ethanol, the electrons in the titania are prevented from recombination with the holes, driving further production of electron-hole pairs¹⁸.

³⁴ In addition to preventing electron-hole pair recombination, ethanol, when functioning as an SED, will produce hydrogen protons when it consumes the produced holes. These hydrogen protons will aid in the methylene blue degradation as the protons are necessary for the breakdown of the ring structure following the *N*-demethylation of methylene blue by holes or radical hydroxyls produced in the titania³⁵⁻³⁶ as detailed in Figure 8B. Ethanol's functionality as a SED has been shown to increase rates of photocatalytic degradation of methylene blue.¹⁸

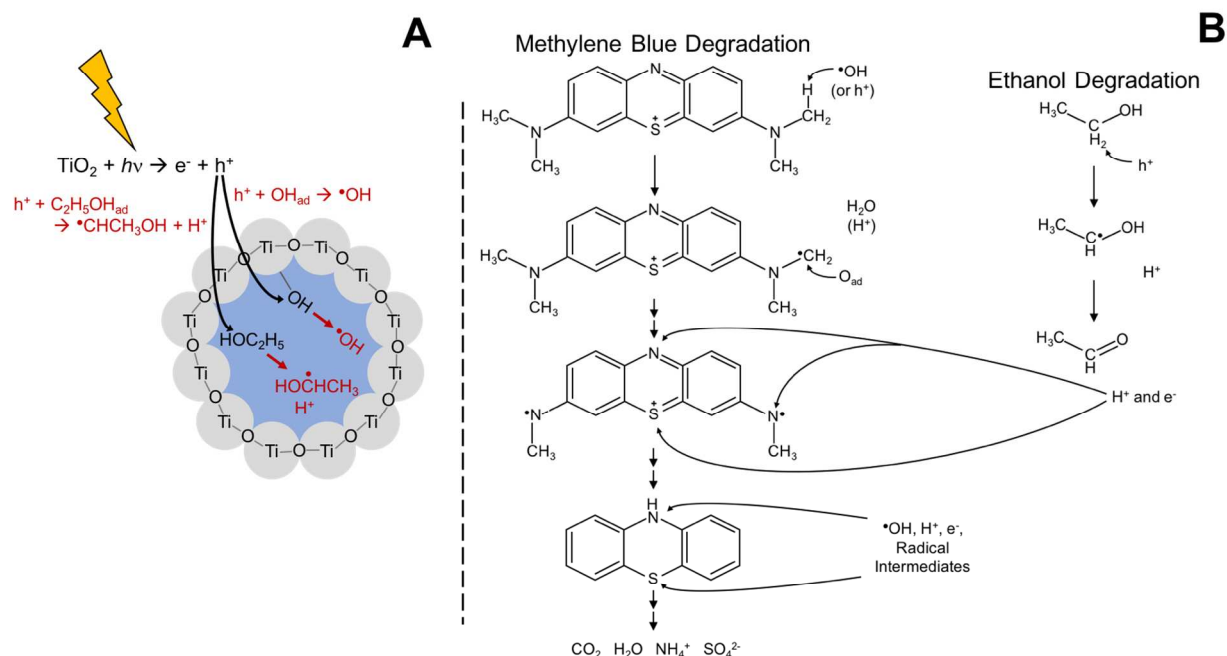


Figure 8. (A) Initiation of photocatalysis in a representative sol-gel-derived titania pore and (B) the following demethylation-initiated methylene blue degradation in the presence of ethanol.

Using ethanol during sol-gel synthesis also leads to potentially positive effects on the structure of the final gel. Ethanol can lead to an increase in surface area within the gel when added during hydrolysis.¹⁴⁻¹⁵ This was illustrated earlier as the 70 and 85 vol% gels had an average porosity of about 87%, whereas the 100 vol% gels had a porosity of 81% as a result of a higher extent of cross-linking. Higher surface area and the resulting higher availability of surface

1
2
3 hydroxyls has been shown to increase photocatalytic efficiency by preventing electron-hole pair
4 recombination as the holes react with the hydroxyls.³⁷⁻³⁹
5
6
7

8 Increased concentrations of ethanol resulted in a higher amount of dye degradation with
9 the crystalline P25, mirroring the results observed with the gels in Figure 6. However, crystalline
10 P25 nanopowder consistently failed to achieve the same level of methylene blue degradation as
11 that seen in the gels. On average, crystalline P25 attained a level of methylene blue concentration
12 or loss at least 12% lower than that observed in the corresponding titania gels. Despite
13 amorphous titania's typically lower photocatalytic activity due to increased band gap energy and
14 the higher potential for electron-hole pair recombination, the gels were able to overcome these
15 limitations. The increased surface area associated with the highly porous titania gels gave an
16 advantage in photocatalytic efficiency over the crystalline P25 nanopowder.
17
18
19
20
21
22
23
24
25
26
27
28

29 To consider the impact of the ethanol as a SED and the porosity difference between the
30 70 and 85 vol% and 100 vol% water gels, the photocatalytic activity of gels synthesized by
31 adding varying amounts of ethanol following the initiation of the polycondensation of the sol
32 were compared to the 70 and 85 vol% water gels. These gels were irradiated with UV light for
33 three hours and the normalized methylene blue concentrations in the gels following treatment are
34 compared in Figure 9. Gels created by adding ethanol after the beginning of polycondensation
35 were expected to have similar porosity to the 100 vol% water gels, but with higher ethanol
36 concentrations in the pores of the gels. The porosity of these new gels was measured and
37 confirmed to be the same as the 100 vol% water gels (see Supporting Information).
38
39
40
41
42
43
44
45
46
47
48
49
50
51
52
53
54
55
56
57
58
59
60

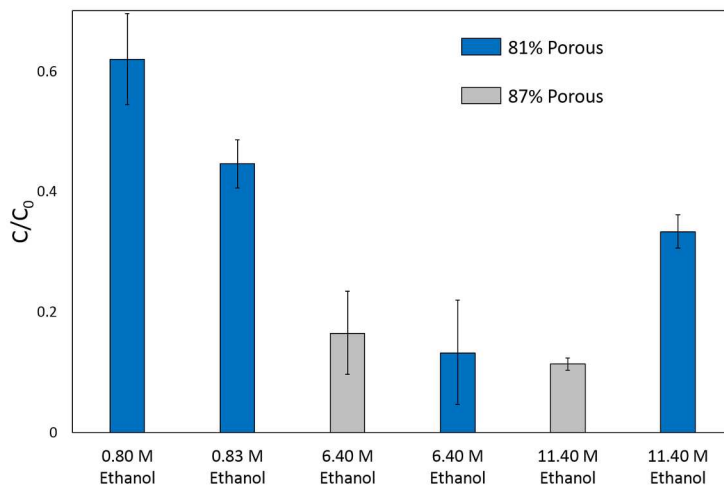


Figure 9. Normalized methylene blue concentration in titania gels by pore ethanol concentration and porosity following 3 hours of UV irradiation. Error bars represent standard deviation.

Even the small addition of only 0.03 M ethanol to the pore liquid of the gels resulted in about 46% more methylene blue degradation than the 100 vol% water gels (0.8 M ethanol). This indicates the extent of SED effects from ethanol at such concentrations within the pores. However, there was no significant difference in performance between gels varying in porosity with an ethanol concentration of 6.4 M. In all cases of ethanol addition, the photocatalytic activity of the gels increased significantly. There does appear to be a limit to how much ethanol can be present in gels of the same porosity before negative effects begin to occur as a result of increasing ethanol. An ethanol concentration of 11.4 M results in a decrease in the extent of methylene blue degradation by 23% when compared to a gel with the same porosity, but a with a concentration 6.4 M of ethanol. Gels with ethanol concentrations of 11.4 M within the pores had varying levels of photocatalytic activity depending on porosity. Gels with a porosity of 81% achieved methylene blue degradation 25% lower than that of gels with porosity of about 87%. In addition to oxidation by photo-generated holes, ethanol can be degraded by radical hydroxyls³⁵ as shown in Figure 10. The competition with the methylene blue for the limited radical hydroxyls

will suppress the dye degradation and would explain the lower performance associated with lower porosity. These results indicate that even very small amounts of ethanol or a similar SED will greatly increase the photocatalytic activity of the titania gels and may be a more controlled method of improving gels without radical synthesis changes necessary to increase gel porosity.

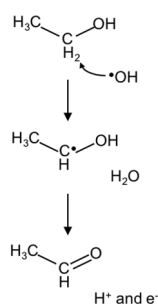


Figure 10. Reaction scheme for radical hydroxyl consumption by ethanol

CONCLUSIONS

Amorphous titania gels were synthesized via a sol-gel protocol that used water as the primary solvent component in order to enhance biomembrane compatibility. Bacteriorhodopsin in its native purple membrane has been successfully encapsulated within titania gels made without ethanol as evidenced by nearly complete retention of the characteristic spectral absorbance over 20 days. BR was shown to reversibly convert to its light-adapted state and to retain its thermochromic behavior once entrapped, indicating that the pores did not hinder the membrane protein's functionality to make conformational changes in response to its environment. This suggests that BR will retain its ability to function as a proton pump, a factor in favor of using the protein over a conventional dye for sensitizing the titania to permit visible light photocatalysis. The amorphous monoliths were photocatalytic at a level comparable with commercial crystalline nanopowders under UV irradiation; almost complete methylene blue dye

1
2
3 degradation was observed within five hours. The inclusion of up to 30 vol% ethanol in the gels
4
5 helped to promote photocatalytic breakdown of the dye. This confirms the capability of ethanol
6
7 to act as a sacrificial electron donor and will be beneficial to the photocatalytic efficiency of
8
9 titania gels once sensitized to visible light for water-splitting hydrogen production. Our future
10
11 work will consider the substitution of ethanol for a less damaging solvent/SED and address the
12
13 incorporation of platinum in the gel-based synthesis of titania-encapsulated bacteriorhodopsin for
14
15 photocatalytic hydrogen production with visible light.
16
17
18
19

20 **AUTHOR INFORMATION**

21 **Corresponding Author**

22
23
24
25 *E-mail: mllongo@ucdavis.edu
26

27 **ACKNOWLEDGEMENTS**

28
29
30 MLL, SHR, KEJ, and SG acknowledge partial support from the National Science Foundation
31
32 under award number DMR-1500275. SHR also acknowledges partial support derived from his
33
34 Blacutt-Underwood Endowed Chair funds. We are grateful to the laboratories of Prof. Karen
35
36 McDonald and Prof. Michael Toney for the use of their UV-Visible spectrophotometers.
37
38
39

40 **ASSOCIATED CONTENT**

41
42 **Supporting Information.** The Supporting Information contains additional details regarding the
43
44 methods used to determine the effects of porosity and ethanol on the photocatalytic efficiency of
45
46 the titania gels. The methods used to determine the band gap energy of the materials, ethanol
47
48 concentrations within the gel pore and final gel porosity are also described. Details of statistical
49
50 analysis and Gaussian regression fitting of UV/Vis spectral data are provided. The Supporting
51
52 Information includes supplemental data related to the thermochromic behavior of BR when in
53
54 solution. This is available free of charge on the ACS Publications website at <http://pubs.acs.org>.
55
56
57
58
59
60

REFERENCES

- (1) Liu, L.; Chen, X. Titanium Dioxide Nanomaterials: Self-Structural Modifications. *Chem. Rev.* **2014**, *114*, 9890-9918.
- (2) Fujishima, A.; Rao, T. N.; Tryk, D. A. Titanium Dioxide Photocatalysis. *J. Photochem. Photobiol., C* **2001**, *1*, 1-21.
- (3) Balasubramanian, S.; Wang, P.; Schaller, R. D.; Rajh, T.; Rozhkova, E. A. High-Performance Bioassisted Nanophotocatalyst for Hydrogen Production. *Nano Lett.* **2013**, *13*, 3365-3371.
- (4) Reisner, E.; Powell, D. J.; Cavazza, C.; Fontecilla-Campes, J. C.; Armstrong, F. A. Visible Light-Driven H₂ Production by Hydrogenases Attached to Dye-Sensitized TiO₂ Nanoparticles. *J. Am. Chem. Soc.* **2009**, *131*, 18457-18466.
- (5) Allam, N. K.; Yen, C.-W.; Near, R. D.; El-Sayed, M. A. Bacteriorhodopsin/TiO₂ Nanotube Arrays Hybrid System for Enhanced Photoelectrochemical Water Splitting. *Energy Environ. Sci.* **2011**, *4*, 2909-2914.
- (6) Hambourger, M.; Brune, A.; Gust, D.; Moore, A. L.; Moore, T. A. Enzyme-Assisted Reforming of Glucose to Hydrogen in Photoelectrochemical Cell. *Photochem. Photobiol.* **2005**, *81*, 1015-1020.
- (7) Chen, X.; Shen, S.; Guo, L.; Mao, S. S. Semiconductor-based Photocatalytic Hydrogen Generation. *Chem. Rev.* **2010**, *110*, 6503-6570.
- (8) Moser, J.; Grätzel, M. Photosensitized Electron Injection in Colloidal Semiconductors. *J. Am. Chem. Soc.* **1984**, *106*, 6557-6564.
- (9) Chu, L.-K.; Yen, C.-W.; El-Sayed, M. A. Bacteriorhodopsin-Based Photo-Electrochemical Cell. *Biosens. Bioelectron.* **2010**, *26*, 620-626.

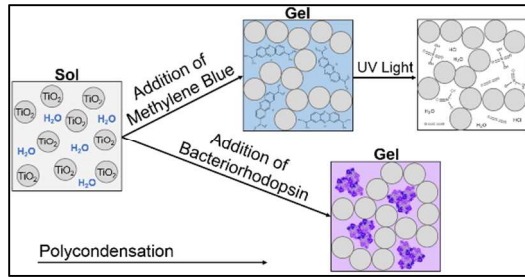
- 1
2
3 (10) Subramaniam, S.; Henderson, R. Molecular Mechanism of Vectorial Proton
4 Translocation by Bacteriorhodopsin. *Nature*. **2000**, *406*, 653-657.
5
6
7
8 (11) Buddee, S.; Wongnawa, S.; Sirimahachai, U.; Puetpaibool, W. Recyclable UV and
9 Visible Light Photocatalytically Active Amorphous TiO₂ Doped with M (III) Ions (M =
10 Cr and Fe). *Mater. Chem. Phys.* **2011**, *126*, 167-177.
11
12
13
14
15 (12) Kaur, K.; Singh, C. V. Amorphous TiO₂ as a Photocatalyst for Hydrogen Production: A
16 DFT Study of Structural and Electronic Properties. *Energy Procedia*. **2012**, *29*, 291-299.
17
18
19
20 (13) Kanna, M.; Wongnawa, S. Mixed Amorphous and Nanocrystalline TiO₂ Powders
21 Prepared by Sol-Gel Method: Characterization and Photocatalytic Study. *Mater. Chem.*
22 *Phys.* **2008**, *110*, 166-175.
23
24
25
26
27 (14) Brinker, C. J.; Scherer, G. W. *Sol-Gel Science: The Physics and Chemistry of Sol-Gel*
28 *Processing*. Academic Press, Inc.: San Diego, CA, 1990.
29
30
31
32 (15) Pierre, A. C. *Introduction to Sol-Gel Processing*. Springer: New York, 1998.
33
34 (16) Kikukawa, T.; Araiso, T.; Shimozawa, T.; Mukasa, K.; Kamo, N. Restricted Motion of
35 Photoexcited Bacteriorhodopsin in Purple Membranes Containing Ethanol. *Biophys. J.*
36 **1997**, *73*, 357-366.
37
38
39
40
41 (17) Houas, A.; Lachheb, H.; Ksibi, M.; Elaloui, E.; Guillard, C.; Herrmann, J.-M.
42 Photocatalytic Degradation Pathway of Methylene Blue in Water. *Appl. Catal., B*. **2001**,
43 *31*, 145-157.
44
45
46
47
48 (18) Konstantinou, I. K.; Albanis, T. A. TiO₂-Assisted Photocatalytic Degradation of Azo
49 Dyes in Aqueous Solution: Kinetic and Mechanistic Investigations A Review. *Appl.*
50 *Catal., B*. **2004**, *49*, 1-14.
51
52
53
54
55
56
57
58
59
60

- 1
2
3
4
5
6
7
8
9
10
11
12
13
14
15
16
17
18
19
20
21
22
23
24
25
26
27
28
29
30
31
32
33
34
35
36
37
38
39
40
41
42
43
44
45
46
47
48
49
50
51
52
53
54
55
56
57
58
59
60
- (19) López, R.; Gómez, R. Band-gap Energy Estimation from Diffuse Reflectance Measurements on Sol-gel and Commercial TiO₂: A Comparative Study. *J. Sol-Gel Sci. Technol.* **2012**, *61*, 1-7.
- (20) Graf, C.; Ohser-Wiedemann, R.; Kreisel, G. Preparation and Characterization of Doped Metal-Supported TiO₂-Layers. *J. Photochem. Photobiol., A* **2007**, *188*, 226-234.
- (21) Hench, L. L.; West, J. K. The Sol-Gel Process. *Chem. Rev.* **1990**, *90*, 33-72.
- (22) Fardad, M. A.; Yeatman, E. M.; Dawney, E. J. C.; Green, M.; Horowitz, F. Effects of H₂O on Structure of Acid-Catalysed SiO₂ Sol-Gel Films. *J. Non-Cryst. Solids.* **1995**, *183*, 2260-267.
- (23) Mitaku, S. I., K.; Itoh, H.; Kataoka, R.; Naka, M.; Yamada, M.; Suwa, M. Denaturation of Bacteriorhodopsin by Organic Solvents. *Biophys. Chem.* **1988**, *30*, 69-79.
- (24) Neebe, M.; Rhinow, D.; Schromczyk, N.; Hampp, N. A. Thermochromism of Bacteriorhodopsin and Its pH Dependence. *J. Phys. Chem. B.* **2008**, *112*, 6946-6951.
- (25) Birge, R. R. Photophysics and Molecular Electronic Applications of the Rhodopsins *Annu. Rev. Phys. Chem.* **1990**, *41*, 683-733.
- (26) Pal, U.; Ghosh, S.; Chatterjee, D. Effect of Sacrificial Electron Donors on Hydrogen Generation over Visible Light-irradiated Nonmetal-doped TiO₂ Photocatalysts. *Transition Met. Chem.* **2012**, *37*, 93-96.
- (27) Scherrer, P. M., M. K.; Sperling, W.; Stoeckenius, W. Retinal Isomer Ratio in Dark-Adapted Purple Membrane and Bacteriorhodopsin Monomers. *Biochem.* **1989**, *28*, 829-834.

- 1
2
3 (28) Hofrichter, J. H., E. R.; Lozier, R. H. Photocycles of Bacteriorhodopsin in Light- and
4 Dark-Adapted Purple Membrane Studied by Time-Resolved Absorption Spectroscopy.
5
6 *Biophys. J.* **1989**, *56*, 693-706.
7
8
9
10 (29) Wang, J. L., S.; Heyes, C. D.; El-Sayed, M. A. Comparison of the Dynamics of the
11 Primary Events of Bacteriorhodopsin in Its Trimeric and Monomeric State. *Biophys. J.*
12
13 **2002**, *83*, 1557-1566.
14
15
16
17 (30) Sonar, S. P., N.; Fischer, W.; Rothschild, K. J. Cell-Free Synthesis, Functional Refolding,
18 and Spectroscopic Characterization of Bacteriorhodopsin, and Integral Membrane
19 Protein. *Biochemistry* **1993**, *32*, 1377-13781.
20
21
22
23
24 (31) Brennan, J. D. Biofriendly Sol-Gel Processing for the Entrapment of Soluble and
25 Membrane-Bound Proteins: Toward Novel Solid-Phase Assays for High-Throughput
26 Screening. *Acc. Chem. Res.* **2007**, *40*, 827-835.
27
28
29
30
31 (32) Liu, H.; Yuan, J.; Shangguan, W. Photochemical Reduction and Oxidation of Water
32 Including Sacrificial Reagents and Pt/TiO₂ Catalyst. *Energy Fuels.* **2006**, *20*, 2289-2292.
33
34
35
36 (33) Kudo, A.; Miseki, Y. Heterogeneous Photocatalyst Materials for Water Splitting. *Chem.*
37
38 *Soc. Rev.* **2009**, *38*, 253-278.
39
40
41 (34) Simon, T.; Bouchonville, N.; Berr, M. J.; Vaneski, A.; Adrović, A.; Volbers, D.;
42 Wyrwich, R.; Döblinger, M.; Susa, A. S.; Rogach, A. L.; Jäckel, F.; Stolarczyk, J. K.;
43 Feldmann, J. Redox Shuttle Mechanism Enhances Photocatalytic H₂ Generation on Ni-
44 Decorated CdS Nanorods. *Nat. Mater.* **2014**, *13*, 1013-1018.
45
46
47
48 (35) Yu, Z. C., S. S. C. Probing Methylene Blue Photocatalytic Degradation by Adsorbed
49 Ethanol with In Situ IR. *J. Phys. Chem. C.* **2007**, *111*, 13813-13820.
50
51
52
53
54
55
56
57
58
59
60

- 1
2
3
4
5
6
7
8
9
10
11
12
13
14
15
16
17
18
19
20
21
22
23
24
25
26
27
28
29
30
31
32
33
34
35
36
37
38
39
40
41
42
43
44
45
46
47
48
49
50
51
52
53
54
55
56
57
58
59
60
- (36) Zhang, T. O., T.; Aoshima, A.; Hidaka, H.; Zhao, J.; Serpone, N. Photooxidative *N*-Demethylation of Methylene Blue in Aqueous TiO₂ Dispersions under UV Irradiation. *J. Photochem. Photobiol., A* **2001**, *140*, 163-172.
- (37) Simonsen, M. E.; Li, Z.; Søgaard, E. G. Influence of the OH Groups on the Photocatalytic Activity and Photoinduced Hydrophilicity of Microwave Assisted Sol-Gel TiO₂ Film. *Appl. Surf. Sci.* **2009**, *255*, 8054-8062.
- (38) Yu, J.; Yu, J. C.; Ho, W.; Jiang, Z. Effects of Calcination Temperature on the Photocatalytic Activity and Photo-Induced Super-Hydrophilicity of Mesoporous TiO₂ Thin Films. *New J. Chem.* **2002**, *26*, 607-613.
- (39) Oosawa, Y.; Grätzel, M. Effect of Surface Hydroxyl Density on Photocatalytic Oxygen Generation in Aqueous TiO₂ Suspensions. *J. Chem. Soc., Faraday Trans. I.* **1988**, *84*, 197-205.

1
2
3
4
5
6
7
8
9
10
11
12
13
14
15
16
17
18
19
20
21
22
23
24
25
26
27
28
29
30
31
32
33
34
35
36
37
38
39
40
41
42
43
44
45
46
47
48
49
50
51
52
53
54
55
56
57
58
59
60



TOC Graphic